

Space-Time Modulated Loaded-Wire Metagratings for Magnetless Nonreciprocity and Near-Complete Frequency Conversion

Yakir Hadad*

School of Electrical Engineering, Tel-Aviv University, Ramat-Aviv, Tel-Aviv, Israel, 69978

Dimitrios Sounas

*Department of Electrical and Computer Engineering,
Wayne State University, Detroit, MI 48202, USA*

(Dated: November 23, 2021)

In recent years a significant progress has been made in the development of magnet-less non-reciprocity using space-time modulation, both in electromagnetics and acoustics. This approach has so far resulted in a plethora of non-reciprocal devices, such as isolators and circulators, over different parts of the spectrum, for guided waves. On the other hand, very little work has been performed on non-reciprocal devices for waves propagating in free space, which can also have many practical applications. For example, it was shown theoretically that non-reciprocal scattering by a metasurface can be obtained if the surface-impedance operator is continuously modulated in space and time. However, the main challenge in the realization of such a metasurface is due to the high complexity required to modulate in space and time many sub-wavelength unit-cells of which the metasurface consists. In this paper we show that spatiotemporally modulated metagratings can lead to strong nonreciprocal responses, despite the fact that they are based on electrically-large unit cells. We specifically focus on wire metagratings loaded with time-modulated capacitances. We use the discrete-dipole-approximation and an ad-hoc generalization of the theory of polarizability for time-modulated particles, and demonstrate an effective nonreciprocal anomalous reflection (diffraction) with an efficient frequency conversion. Thus, our work opens a venue towards a practical design and implementation of highly non-reciprocal magnet-less metasurfaces in electromagnetics and acoustics.

PACS numbers: Valid PACS appear here

I. INTRODUCTION

In recent years substantial efforts have been devoted towards the development of magnet-less non-reciprocal devices in electromagnetics as well as in acoustics^{1–10}. In particular, space-time modulated structures have been explored theoretically and experimentally for this purpose^{11–17}. These designs are based on the creation of a synthetic sense of motion¹⁸ that fundamentally enables the breach of time-reversal symmetry *with respect to the guiding-wave sub-system*. While the major part of these efforts has been dedicated to breaking reciprocity in guiding wave structures, some important focus has been also aimed at the violation of reciprocity in scattering and radiation^{19–22}. For example in²⁰ a space-time modulated travelling wave antenna with different radiation patterns in transmit and receive mode was studied theoretically and experimentally. In that antenna, a few voltage varying capacitors were used to establish the required modulation. The underlying idea of this design is to amplify the effect of the spatiotemporal modulation by taking advantage of asymmetric interband transitions between different space-time harmonics of a mode inside and outside the light-cone. Thus, in a sense, the natural sharp filtering property of the light cone has been used to enhance the nonreciprocal effect in this low-Q leaky wave antenna system. In another work¹⁹, a metasurface that consists of a space-time modulated impedance operator has been explored theoretically. In that proposal non-reciprocal

Wood's anomaly has been achieved through a careful design of the space-time modulation of the surface characteristics. However, unlike the antenna in Ref.²⁰ which required a small number of modulation actuators, for the emulation of the effective surface impedance in¹⁹, an unrealistically, extremely complex configuration of voltage varying capacitors and dense wiring system is required to achieve the many different modulation regions.

A possible venue to overcome this issue may be based on using metagratings which are metasurfaces with electrically large unit cells. Metagratings^{23–32}, a close relative of frequency selective surfaces and diffraction gratings, have been explored recently as another means to overcome the challenge of perfect anomalous reflection and refraction by an electrically thin metasurface^{33–49}. As opposed to the traditional metasurface approach in which electrically deep subwavelength unit cells are involved, the unit cell of the metagrating is $\mathcal{O}(\lambda/2)$ or more and thus fundamentally gives rise to propagating diffraction orders. Then, a proper design of the metagrating's unit-cell enables a significant control over the balance of the various propagating diffraction orders, and in particular makes it possible to nullify the zero order harmonic which corresponds to regular reflection and refraction. Moreover, recently, an interesting proposal for a dielectric slab metagrating with space-time modulated refractive index has been explored demonstrating a peculiar relations between the space-time harmonics in this system³². In particular, non-reciprocal scattering has

been theoretically demonstrated. Nonetheless, a realistic implementation of space-time modulated refractive index is challenging and requires either nonlinear media with significant pump power or the use of effective medium, e.g., using a dense array of unit-cells that are loaded by voltage-varying capacitors. Thus, unfortunately raising again the challenge of realizability.

Here, inspired by the recent progress in metagratings^{23–32}, we propose a solution to this problem and design efficient non-reciprocal metasurfaces by using only a minimal number of *three* distinct modulation regions and small modulation parameters. Specifically, we develop a rigorous theory for metagratings with time-modulated resonant elements. Using this approach we explore analytically a two-dimensional lattice of resonant, capacitively loaded, wires that are subject to space-time modulation. To that end we first develop a generalization of polarizability theory for time-modulated particles, and later exploit it together with the discrete-dipole approximation^{50–55} and the proper Green's function to explore analytically the scattering from an infinite space-time modulated metagratings. We particularly show that non-reciprocal anomalous reflection can be achieved with nearly perfect coupling efficiency between the incident wave and the desired scattered wave. As opposed to anomalous reflection obtained by a stationary metagratings, here, the anomalous reflection process involves also an efficient frequency conversion process.

II. THE GENERALIZED POLARIZABILITY OF TIME-MODULATED LOADED WIRE

Consider a periodically loaded perfect electrically conducting (PEC) wire that is co-aligned with the z -axis as illustrated in Fig. 1(a). The wire radius is r_0 , the loading impedance is Z_L , and the loading periodicity is small on the wavelength, i.e., $\Delta \ll \lambda$. Now let $\mathbf{E}(\omega) = \hat{z}E(\omega)$ be the electric field at the wire location but in the absence of the wire itself. Then, the induced current on the wire is given by⁵¹

$$I(\omega) = \alpha(\omega)E(\omega) \quad (1)$$

with the effective susceptibility⁵⁶ α ,

$$\alpha^{-1}(\omega) = \alpha_0^{-1}(\omega) + \frac{Z_L}{\Delta} \quad (2)$$

where

$$\alpha_0^{-1}(\omega) = \frac{\eta k}{4} H_0^{(2)}(kr_0) \quad (3)$$

is the susceptibility of an unloaded PEC wire. In Eq. (3), $\eta = 120\pi\Omega$ and $k = \omega/c$ are the free space impedance and wavenumber, respectively. Also, ω is the radial frequency, c is the speed of light in vacuum, and $H_0^{(2)}$ is

zero order Hankel function of the second kind. To simplify subsequent notations, in the following we use

$$\gamma(\omega) = \frac{1}{\alpha(\omega)}. \quad (4)$$

Then, for *capacitive* periodic loading we can write

$$\gamma(\omega) = \gamma_0(\omega) + \frac{1}{j\omega C\Delta} \quad (5)$$

where C is the per-unit-length loading capacitance.

Up to this point the formulation has been strictly carried out in the frequency domain. However, in the following we shall introduce temporal modulation of the loading capacitor. We assume

$$\frac{1}{C(t)} = \frac{1}{C_0} [1 + m \cos(\omega_m t + \phi)], \quad (6)$$

where ω_m is the modulation frequency, m is the modulation index and ϕ is the modulation phase shift between the wires in the meta-grating structure. To model the scattering process in this case it is required to repeat the previous derivation, but in the time-domain. To that end we use the convolution property of the Fourier transform on Eq. (1) with Eq. (4). We have

$$\mathcal{E}(t) = \gamma(t) * \mathcal{I}(t) = \int_{-\infty}^{\infty} \gamma(\tau) \mathcal{I}(t - \tau) d\tau \quad (7)$$

where $\mathcal{E}(t)$, $\gamma(t)$, and $\mathcal{I}(t)$ are the time domain counterparts of $E(\omega)$, $\gamma(\omega)$, and $I(\omega)$, respectively, and $*$ denotes convolution as defined in Eq. (7). By explicitly expanding Eq. (7) using Eq. (5), we get

$$\mathcal{E}(t) = \gamma_0(t) * \mathcal{I}(t) + \frac{1}{\Delta C(t)} \mathcal{F}^{-1} \left\{ \frac{I(\omega)}{j\omega} \right\} (t) \quad (8)$$

$$= \gamma_0(t) * \mathcal{I}(t) + \frac{1}{\Delta C(t)} \int_{-\infty}^t \mathcal{I}(\tau) d\tau \quad (9)$$

Here \mathcal{F}^{-1} stand for the inverse Fourier transform. In the last equality we used the identity $\mathcal{F}^{-1}\{I(\omega)/j\omega\} = \int_{-\infty}^t \mathcal{I}(\tau) d\tau - 0.5I(\omega)|_{\omega=0}$, together with the fact $I(\omega)|_{\omega=0} = 0$ (implying no DC currents in the problem).

Assuming that the exciting field is harmonic at frequency ω , then, due to modulation at ω_m , the induced current and the electric field in the problem may be expressed by

$$\mathcal{X}(t) = \frac{1}{2} \sum_{n=-\infty}^{\infty} \mathcal{X}_n e^{j\omega_n t} + c.c. \quad (10)$$

where \mathcal{X} stands for either \mathcal{I} or \mathcal{E} , and \mathcal{X}_n denotes the complex coefficient of n 'th harmonic at $\omega_n = \omega + n\omega_m$. Next, in order to obtain a difference equation that relates between the different harmonics of the exciting electric field and the induced current, we apply Eq. (10) in

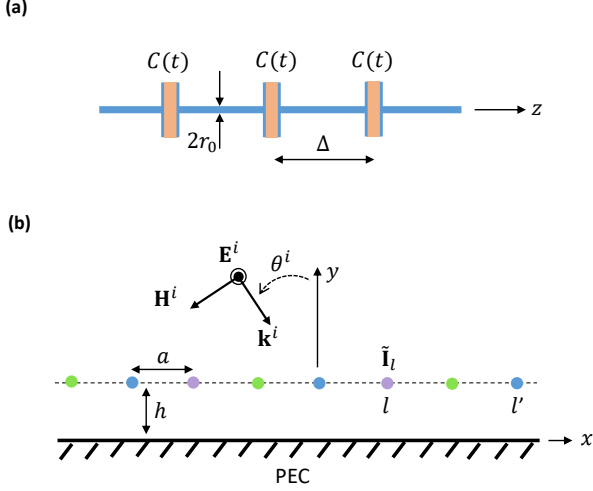


FIG. 1. Illustration of the problem. (a) Temporally modulated capacitively loaded wire, co-aligned with the z -axis. (b) A space time modulated metagratings wire array above a perfect electrically conducting plate. Here, the spatial periodicity is $N = 3$, the minimal required to achieve non-reciprocity by synthetic motion.

Eq. (8). Beginning with the last term in Eq. (8), we find after a simple derivation,

$$\frac{1}{C(t)} \int_{-\infty}^t \mathcal{I}(\tau) d\tau = \frac{1}{2C_0} \sum_{n=-\infty}^{\infty} e^{j\omega_n t} \left[\frac{\mathcal{I}_n}{j\omega_n} + \frac{m}{2} e^{j\phi} \frac{\mathcal{I}_{n-1}}{j\omega_{n-1}} + \frac{m}{2} e^{-j\phi} \frac{\mathcal{I}_{n+1}}{j\omega_{n+1}} \right] + c.c. \quad (11)$$

Next, we evaluate the first term in Eq. (8). To that end we use the convolution identity

$$\gamma_0(t) * \mathcal{I}(t) = \mathcal{F}^{-1} \{ \gamma_0(\omega) \mathcal{I}(\omega) \} \quad (12)$$

with the Fourier transform of Eq. (10) (here, $\mathcal{X} = \mathcal{I}$)

$$\mathcal{I}(\omega) = \frac{1}{2} \sum_{n=-\infty}^{\infty} \mathcal{I}_n \delta(\omega - \omega_n) + c.c. \quad (13)$$

Therefore leading to

$$\gamma_0(t) * \mathcal{I}(t) = \frac{1}{2} \sum_{n=-\infty}^{\infty} \mathcal{I}_n \gamma_0(\omega_n) e^{j\omega_n t} + c.c. \quad (14)$$

Finally, by combining Eqs. (14) and (11) in Eq. (8) and with Eq. (10), we get

$$\mathcal{E}_n = \mathcal{I}_n \gamma_0(\omega_n) + \frac{1}{\Delta C_0} \left[\frac{\mathcal{I}_n}{j\omega_n} + \frac{m}{2} e^{j\phi} \frac{\mathcal{I}_{n-1}}{j\omega_{n-1}} + \frac{m}{2} e^{-j\phi} \frac{\mathcal{I}_{n+1}}{j\omega_{n+1}} \right]. \quad (15)$$

Using Eq. (15) it is possible to define a “generalized” effective susceptibility $\underline{\alpha}$ for time-modulated wires. In this case, α becomes a matrix that relates between the electric field and the induced currents in different harmonics. For example, if we choose to take into account only three harmonics, $n = 0, \pm 1$, that is at $\omega_0 = \omega, \omega_{\pm 1} = \omega \pm \omega_m$ we get

$$\tilde{\mathbf{I}} = \underline{\alpha} \tilde{\mathbf{E}} \quad (16)$$

where $\tilde{\mathbf{E}} = [\mathcal{E}_{-1}, \mathcal{E}_0, \mathcal{E}_1]^T$ and $\tilde{\mathbf{I}} = [\mathcal{I}_{-1}, \mathcal{I}_0, \mathcal{I}_1]^T$, and

$$\underline{\alpha}^{-1} = \begin{bmatrix} \gamma_0(\omega_{-1}) + \frac{1}{j\Delta C_0 \omega_{-1}} & \frac{me^{-j\phi}}{2j\Delta C_0 \omega_0} & 0 \\ \frac{me^{j\phi}}{2j\Delta C_0 \omega_{-1}} & \gamma_0(\omega_0) + \frac{1}{j\Delta C_0 \omega_0} & \frac{me^{-j\phi}}{2j\Delta C_0 \omega_1} \\ 0 & \frac{me^{j\phi}}{2j\Delta C_0 \omega_0} & \gamma_0(\omega_1) + \frac{1}{j\Delta C_0 \omega_1} \end{bmatrix} \quad (17)$$

III. A LINEAR ARRAY OF TIME-MODULATED CAPACITIVELY LOADED WIRES

Consider a linear array of capacitively loaded time-modulated wires, located at $y = h$, above an infinite PEC plate that is placed on the $y = 0$ plane. The inter-wire spacing is a and the wires are loaded with capacitors $C(t)$, as in Eq. (6), with

$$\phi = -\frac{2\pi l}{N} \quad (18)$$

where $l \in \mathbb{Z}$ is the wire index and N is the spatial periodicity. For simplicity, in the following we shall assume that $N = 3$, which is the minimal spatial periodicity that is required to achieve the effect of a synthetic motion, and thus, non-reciprocity. An illustration of the structure in this case is shown in Fig. 1(b).

A. Formulation of the excitation dynamics

The lattice is excited by an impinging plane wave

$$\mathbf{E}^i(\mathbf{r}; \omega) = \hat{z} E^i e^{-j\mathbf{k}^i \cdot \mathbf{r}} \quad (19)$$

where $\mathbf{r} = (x, y)$, $\mathbf{k}^i = (k_x^i, -k_y^i)$ where $k_x^i = k \sin \theta^i$ and $k_y^i = k \cos \theta^i$ and with $-90^\circ < \theta^i < 90^\circ$ being the angle of incidence with respect to the normal \hat{y} . Clearly, θ^i is positive (negative) for waves with positive (negative) k_x component of the wavenumber. See Fig. 1(b).

Using the generalized time-modulated susceptibility concept developed in the previous section, the equation of dynamics for the infinite array can be expressed as

$$\underline{\alpha}_l^{-1} \tilde{\mathbf{I}}_l = \tilde{\mathbf{E}}^i(\mathbf{r}_l) + \sum_{l' \neq l} \underline{G}(|\mathbf{r}_l - \mathbf{r}_{l'}|) \tilde{\mathbf{I}}_{l'} - \sum_{l'} \underline{G}(|\mathbf{r}_l - \mathbf{r}_{l'}^i|) \tilde{\mathbf{I}}_{l'}. \quad (20)$$

Here $\underline{\alpha}_l$ is the generalized susceptibility of the l -th wire, and \underline{G} is the two-dimensional free-space Green's function evaluated at each of the intermodulation frequencies. Thus, in general,

$$\underline{G} = \text{diag}[\dots, G_{n-1}, G_n, G_{n+1}, \dots] \quad (21)$$

where

$$G_n(|r - r'|) = \frac{-\eta k_n}{4} H_0^{(2)}(k_n |r - r'|) \quad (22)$$

with $k_n = \omega_n/c$, and $\mathbf{r} = (x, y)$, $\mathbf{r}' = (x', y')$ are the locations of the observer and the source, respectively. In Eq. (20) $r_l = (h, la)$ is the locations of the l -th wire on the (x, y) plane, and $r_l^i = (-h, la)$ is the location of the *image* by the PEC plate of the l -th wire. Thus, in Eq. (20) we use image theory in order to replace the original problem with a new problem in which all the wires are located in free space. For this reason, the generalized susceptibility developed in the previous section for a wire in free-space is still valid. However, it is essential to write correctly the incident field in this case. The latter consists of the impinging wave which is given in Eq. (19), plus the reflected wave from the PEC plate in the absence of the wire array. Specifically, on $\mathbf{r}_l = (al, h)$ for the case of $N = 3$, and after taking into account only the three low order harmonics $n = 0, \pm 1$, the incident field in Eq. (20) reads,

$$\tilde{\mathbf{E}}^i(\mathbf{r}_l) = [0, 2jE^i \sin(k_y^i h) e^{-jk_x^i al}, 0]^T \quad (23)$$

highlighting the fact that there are no intermodulation frequencies in the incident wave.

B. The induced currents

Due to Floquet-Bloch theorem, the n -th harmonic of the induced current on the l -th wire is given by

$$\mathcal{I}_{n,l} = \mathcal{A}_n e^{-j\psi_n l} \quad (24)$$

where

$$\psi_n = k_x^i a + \frac{2\pi n}{3}. \quad (25)$$

Consistent with previous approximation of weak temporal modulation, we keep only the three fundamental harmonics, $n = 0, \pm 1$, and write,

$$\tilde{\mathbf{I}}_l = [\mathcal{I}_{-1,l}, \mathcal{I}_{0,l}, \mathcal{I}_{1,l}]^T. \quad (26)$$

This solution ansatz is applied in the infinite summations of Eq. (20). Beginning with the first summation in Eq. (20), for a specific harmonic n , and following similar derivation as in⁵¹, we have

$$\sum_{l' \neq l} G_n(|\mathbf{r}_l - \mathbf{r}_{l'}|) \mathcal{I}_{n,l'} = 2\mathcal{A}_n e^{-j\psi_n l} \left(-\frac{\eta k_n}{4} \right) S_1^{(n)} \quad (27)$$

where

$$S_1^{(n)} = \sum_{s=1}^{\infty} H_0^{(2)}(k_n a s) \cos(\psi_n s) = \frac{1}{\beta_{0n} a} - \frac{1}{2} + \frac{j}{\pi} \left[\ln \left(\frac{k_n a}{4\pi} \right) + \gamma + \frac{1}{2} \sum_{m \neq 0} \left(\frac{-2\pi j}{\beta_{mn} a} - \frac{1}{|m|} \right) \right] \quad (28)$$

and with

$$\beta_{mn} = \sqrt{k_n^2 - \left(\frac{2\pi m}{a} + \frac{\psi_n}{a} \right)^2}, \quad \Im\{\beta_{mn}\} \leq 0. \quad (29)$$

The second summation in Eq. (20) is treated using a conventional Poisson summation as in⁵¹.

$$\sum_{l'} G_n(|\mathbf{r}_l - \mathbf{r}_{l'}^i|) \mathcal{I}_{n,l'} = \mathcal{A}_n e^{-j\psi_n l} \left(-\frac{\eta k_n}{4} \right) S_2^{(n)} \quad (30)$$

where

$$S_2^{(n)} = \sum_{s=-\infty}^{\infty} H_0^{(2)}(k_n \sqrt{|s|^2 a^2 + 4h^2}) e^{j\psi_n s} = \frac{2}{a} \sum_{m=-\infty}^{\infty} \frac{e^{-j2\beta_{mn} h}}{\beta_{mn}} \quad (31)$$

with β_{mn} as defined in Eq. (29). Once the summations are evaluated, using Eq. (20) it is possible to write an equation for the unknown excitation amplitudes \mathcal{A}_n . Consistent with previous notations we denote

$$\tilde{\mathbf{A}} = [\dots, \mathcal{A}_{n-1}, \mathcal{A}_n, \mathcal{A}_{n+1}, \dots]^T. \quad (32)$$

Taking into account only three harmonics $n = 0, \pm 1$, we end up with solving the following linear equation for the excitation amplitudes at each harmonics,

$$(\underline{M} - \underline{R}) \tilde{\mathbf{A}} = \tilde{\mathbf{E}}^i(\mathbf{r}_0) \quad (34)$$

with

$$\underline{\underline{M}} = \begin{bmatrix} \gamma_0(\omega_{-1}) + \frac{1}{j\Delta C_0\omega_{-1}} & \frac{m}{2j\Delta C_0\omega_0} & 0 \\ \frac{m}{2j\Delta C_0\omega_{-1}} & \gamma_0(\omega_0) + \frac{1}{j\Delta C_0\omega_0} + \frac{m}{2j\Delta C_0\omega_1} & \frac{m}{2j\Delta C_0\omega_1} \\ 0 & \frac{m}{2j\Delta C_0\omega_0} & \gamma_0(\omega_1) + \frac{1}{j\Delta C_0\omega_1} \end{bmatrix} \quad (35)$$

and

$$\underline{\underline{R}} = \frac{\eta}{4} \text{diag}[k_{-1}S^{(-1)}, k_0S^{(0)}, k_1S^{(1)}] \quad (36)$$

and $\tilde{\mathbf{E}}^i(\mathbf{r}_0) = \tilde{\mathbf{E}}^i(\mathbf{r}_l)$ of Eq. (23) at $l = 0$.

C. The total fields

The total fields contain different contributions from the impinging and reflected wave by the PEC plate, as well as, of course, by the scattering due to the wires. Thus, the total field at the n -th harmonic reads

$$E_{z,n} = E^i e^{-j(k_x^i x - k_y^i y)} - E^i e^{-j(k_x^i x + k_y^i y)} + \frac{\eta k_n}{4} \mathcal{A}_n \sum_{l=-\infty}^{\infty} \left[H_0^{(2)} \left(k_n \sqrt{(x-la)^2 + (y-h)^2} \right) e^{-j\psi_n l} - H_0^{(2)} \left(k_n \sqrt{(x-la)^2 + (y+h)^2} \right) e^{-j\psi_n l} \right] \quad (37)$$

After applying Poisson summation and separating between the specular reflection term and the higher diffraction harmonics, the total field above $y = h$ are given by

$$E_{z,n} = E^i e^{-j(k_x^i x - k_y^i y)} \delta_n + \sum_{m=-\infty}^{\infty} E_{mn}^r e^{-j(k_{x,mn} x + \beta_{mn} y)} \quad (38)$$

with

$$E_{mn}^r = -E^i \delta_n - \frac{j\eta k_n \sin(\beta_{mn} h)}{\beta_{mn} a} \mathcal{A}_n \quad (39)$$

where δ_n is the delta of Kronecker, $\delta_n = 1$ for $n = 0$ and $\delta_n = 0$ otherwise, \mathcal{A}_n is found as a solution to Eq. (34), and $k_{x,mn}$ and β_{mn} are the x and y components of the propagation wavevector. The former is given by

$$k_{x,mn} = \frac{2\pi m}{a} + \frac{\psi_n}{a} \quad (40)$$

whereas the latter by Eq. (29). Clearly, $k_{x,mn}$ and β_{mn} satisfy the free-space dispersion relation $k_{x,mn}^2 + \beta_{mn}^2 = k_n^2$.

D. Space-time diffraction orders

From Eq. (38) together with Eq. (29) it is clear that in the space-time modulated metagrating structure, diffraction lobes are a consequence of the geometrical periodicity a as well as of the spatial and temporal modulation

periodicity. Specifically, propagating diffraction order of spatial order m and temporal order n will exists if

$$\left| \frac{2\pi}{a} \left[m + \frac{n}{3} \right] + k_x^i \right| < \frac{\omega + n\omega_n}{c} \quad (41)$$

which boils down to either

$$0 \leq m + \frac{n}{3} + \tilde{a} \sin \theta^i \leq \tilde{a} + n\delta\tilde{a} \quad \text{or} \\ -\tilde{a} - n\delta\tilde{a} \leq m + \frac{n}{3} + \tilde{a} \sin \theta^i \leq 0 \quad (42)$$

where $\tilde{a} = a/\lambda$ and $\delta = \omega_m/\omega$. Propagating reflected wave harmonics propagate at angle

$$\theta_{mn} = \sin^{-1}(k_{x,mn}/k_n) \quad (43)$$

measured with respect to the y axis, where for reflected waves θ is defined as positive/negative for wavenumbers in the first/second xy quadrant. Note that for the incoming, impinging wave, the definition is opposite.

Now it is clear that in order to cancel specular reflection at the incident wave frequency it is required to nullify, or at least minimize, the following term that consists of the specular reflection by the PEC plate and the $n = 0$ temporal harmonic of the $m = 0$ spatial harmonic. That is,

$$-E^i - \frac{j\eta k \sin(k_y^i h)}{a k_y^i} A_0 = 0 \quad (44)$$

where A_0 is given by solving Eq. (34).

E. Energy balance

The net power flux carried by the mn propagating reflected harmonics through the $y = h$ plane is given by

$$S_{mn} = \cos \theta_{mn} \frac{|E_{mn}^r|^2}{\eta}. \quad (45)$$

In a lossless, passive, and stationary metagratings system it is required that the net outgoing flux will be equal to the net incoming flux by the impinging wave. In our system, however, due to the parametric process of the temporal modulation, some additional energy may

be pumped into or extracted from the wave system^{57–61}. Thus, in our system the energy balance reads

$$\Delta S_{mod} + S_{inc} - \sum_{(mn) \in prop} S_{mn} = 0 \quad (46)$$

Nonetheless, since the modulation frequency is small compared to the signal frequency, this exceed power is expected to be relatively small, thus $\Delta S_{mod} \ll S_{inc}$.

IV. NONRECIPROCAL ANOMALOUS REFLECTION WITH NEAR COMPLETE FREQUENCY CONVERSION

In this section we use the theory developed above in order to demonstrate one possible functionality of the time-modulated metagratings surface. We consider a space-time modulated metagratings structure with the following parameters: reference frequency f_r , reference wavelength $\lambda_r = c/f_r$, inter-wire distance $a = 0.6\lambda_r$, wires distance from the PEC plate h , wire loading capacitance $C_0 = 1\text{pF}$, loading periodicity $\Delta = 0.1\lambda_r$, and wire radius $r_0 = 0.5\text{mm}$. We introduce space-time modulation of the wires in the lattice such that $\omega_m = 0.1\omega_r$ ($\omega_r = 2\pi f_r$) with modulation index $m = 0.1$, and super-cell size $N = 3$. A stationary metagratings structure, namely, in the absence of the space-time modulation, has been shown to be able to completely nullify the specular reflection^{23–31}. Instead, the energy is directed to one of the grating lobes of the structure. This functionality has been recently termed - anomalous reflection. Nonetheless, up to now this effect has been demonstrated only in reciprocal structures, with the exception in³² which explored a metagrating dielectric slab with a continuous space-time modulation of the refractive index. Due to reciprocity, if an impinging wave at θ^i is fully reflected to θ^r , then a wave arriving at $-\theta^r$ will be reflected with the same efficiency to $-\theta^i$, where θ^i and θ^r are measured with respect to the y axis, *and* considered positive when corresponding to waves with positive k_x component of the wave number. Here, we show that upon space-time modulation this effect can be turned to be strongly non-reciprocal, and moreover, we demonstrate that even with a small modulation index it is possible to achieve a near complete frequency conversion by the temporal modulation.

With the parameters listed above, in Fig. 2 we show the suppression of the specular reflection as a function of the incidence angle θ^i and the distance between the lattice and the PEC plate h . The figure shows the specular reflection intensity, color-coded in logarithmic scale. For large range of parameters nearly full reflection takes place. However, at certain regions in the reflection intensity map inter-harmonic resonances take place leading to full suppression on the specular reflection. From the asymmetry in the figure, it is clear that this effect is non-reciprocal, leading to a very different power transmission for impinging waves that are coming from complementary

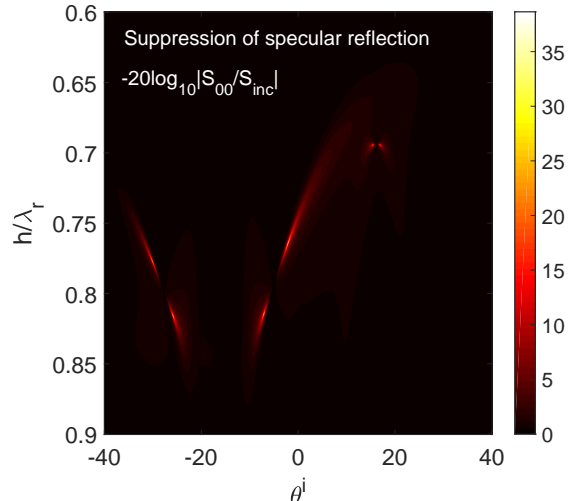


FIG. 2. Suppression of the specular reflection [in dB] as function of the incident wave angle θ^i and the spacing h between the wire-lattice and the PEC plate. This map is calculated for the parameters that are listed in the text, specifically, $a/\lambda = 0.6$. In the map, the *dark areas correspond to full specular reflection*, whereas significant suppression of specular reflection is characterized by light colors. In these regions where specular reflection is prohibited, significant frequency conversion takes place into another space-time diffraction order as shown the Fig. 3 below.

direction, θ^i or $-\theta^i$. Let us consider a specific example, with $h = 0.7775\lambda_r$ and incidence angle $\theta^i = -30^\circ$. With these parameters, using Eq. (42) it is clear that besides the specular reflection (fundamental harmonic $(m, n) = (0, 0)$), also the higher order $(m, n) = (1, -1)$ and $(m, n) = (0, 1)$ harmonics are propagating. This means, that the incident wave power that is not specularly reflected has to efficiently couple to one or two of these additional propagating diffraction orders. This is demonstrated in Fig. 3 below. In the figure, the power flux density along the y direction, S_{mn} , is shown for the propagating harmonics. The specular reflection wave due to an incident wave at $\theta^i = -30^\circ$ is shown in blue. At the desired reference frequency, specular reflection is completely suppressed. The incident wave energy experiences practically complete conversion to the $(m, n) = (1, -1)$ harmonic that propagates at frequency $\omega_{-1} = \omega_r - \omega_m$ which is reflected towards $\theta_{(1,-1)} \approx 42^\circ$. As opposed to that, the $(m, n) = (0, 1)$ harmonic which is also propagating is very weakly excited. On the contrary, in the absence of inter-harmonic resonances as shown in Fig. 2, the wave that impinges at the complementary direction, i.e., at $\theta^i = 30^\circ$ experiences nearly complete specular reflection, and therefore, practically, no additional propagating harmonics will be excited.

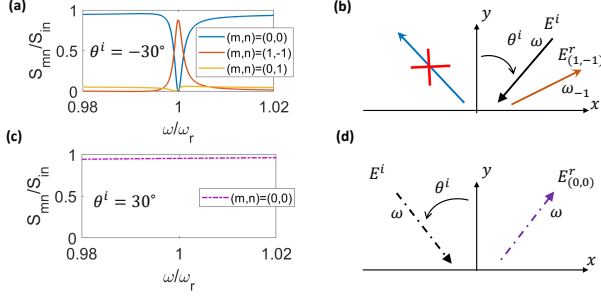


FIG. 3. Non-reciprocal scattering and high efficient frequency conversion. (a) With $\theta^i = -30^\circ$. In this case there is no specular reflection at $\omega = \omega_r$ as shown by the continuous blue line. The dominant reflected wave corresponds to the $(m, n) = (1, -1)$ space time harmonics which propagates at angle $\theta_{1,-1}^r \approx 42^\circ$ and at frequency $\omega_{-1} = \omega - \omega_m$. Due to the parametric modulation some scattering to additional harmonics may take place but with very low efficiencies. For example, an additional propagating harmonics $(m, n) = (0, 1)$ shown in yellow is practically not excited. An illustration of the overall response in this case is shown in (b). As opposed to that, with $\theta^i = 30^\circ$ practically regular specular reflection takes place as shown in (c), with $\theta^r = 30^\circ$. In this case the metagrating surface practically behaves as a simple reflector, as illustrated in (d). Yet, additional scattering harmonics reduce the overall efficiency by some minor extent.

V. SOME PRACTICAL CONSIDERATIONS AND CONCLUSIONS

A few words on practical realization of the proposed design. In the example considered above only $N = 3$ modulation regions are required per unit cell. The distance between the wires is large on the wavelength thus enabling a convenient wiring system. Furthermore, we note that all the capacitors that are distributed on each wire can be modulated simultaneously by modulation voltage that is applied at the two ends of each wire. Moreover, an additional simplification of the practical

implementation may be achieved if each family of wires that are subject to the same modulation (namely, all the wires of the same color in Fig. 1) will be placed at a different height with respect to the ground plane. In that case, the modulation scheme may be designed using even a smaller number of modulation drivers. Note though that the analysis carried out in this paper should be slightly adjusted for this particular case.

To conclude, in this paper we have developed a theoretical model based on the discrete-dipole-approximation and polarizability theory for the scattering by a two-dimensional lattice of space-time modulated resonant capacitively loaded wires. Using this simple methodology we demonstrate the design of a significantly non-reciprocal anomalous reflection using metagrating structure with *electrically large* unit cells that contain a single wire each. Thus, significantly simplifying the practical requirements for the modulation system and hence opening a realistic possibility for actual fabrication of such devices. The non-reciprocal scattering process described here is also associated with efficient frequency conversion of the anomalous refracted beam. While the model explored in this paper involves capacitively loaded wires, the same approach may be also augmented to the optical frequency regime using fast modulation techniques^{62,63}. And with possible implications in radio-frequency devices as well as for more efficient photovoltaic processes^{64,65}. Moreover, we note that the model developed in this paper may be readily augmented to solve the excitation response due to a localized source by taking an approach akin to^{66,67}.

ACKNOWLEDGMENTS

Y. Hadad would like to acknowledge support by the Alon Fellowship granted by the Israeli Council of Higher Education (2018-2021).

* hadady@eng.tau.ac.il

¹ S. Tanaka, N. Shimimura, and K. Ohtake, "Active circulators: The realization of circulators using transistors," *Proc. IEEE*, **53**, (3), pp. 260-267, (1965).

² Y. Ayasli, "Field effect transistor circulators," *IEEE Trans. Magn.*, **25**, (5), pp. 3242-3247, (1989).

³ K. Gallo and G. Assanto, "All-optical diode in a periodically poled lithium niobate waveguide," *Appl. Phys. Lett.*, **79**, (3), pp. 314-316, (2001).

⁴ T. Kodera, D. L. Sounas, and C. Caloz, "Artificial Faraday rotation using a ring metamaterial structure without static magnetic eld," *Appl. Phys. Lett.*, **99**, pp. 03114, (2011).

⁵ D. L. Sounas, T. Kodera, and C. Caloz, "Electromagnetic modeling of a magnetless nonreciprocal gyrotropic metasurface," *IEEE Trans. Antennas Propag.*, **61**, (1), pp. 221-231, (2013).

⁶ Z. Wang, *et al.*, "Gyrotropic response in the absence of a bias field," *Proc. Natl. Acad. Sci. U.S.A.*, **109**, (33), pp. 13194-13197, (2012).

⁷ B.-I. Popa and S. A. Cummer, "Nonreciprocal active metamaterials," *Phys. Rev. B*, **85**, p. 205101, (2012).

⁸ S. Manipatruni, J. T. Robinson, and M. Lipson, "Optical nonreciprocity in optomechanical structures," *Phys. Rev. Lett.*, **102**, 213903, (2009).

⁹ Y. Mazar, A. Alú, "Nonreciprocal hyperbolic propagation over moving metasurfaces," *Phys. Rev. B* **99** (4), 045407 (2019)

¹⁰ R. Fleury, D. L. Sounas, C. F. Sieck, M. R. Haberman, and A. Alú, "Sound isolation and giant linear nonreciprocity in a compact acoustic circulator," *Science*, **343**, pp. 516-519, (2014).

¹¹ S. Qin, Q. Xu, and Y. E. Wang, "Nonreciprocal com-

- ponents with distributedly modulated capacitors,” *IEEE Trans. Microw. Theory Techn.*, **62**, (10), pp. 2260-2272, (2014).
- ¹² N. Reiskarimian and H. Krishnaswamy, “Magnetic-free non-reciprocity based on staggered commutation,” *Nat. Commun.*, **7**, p. 11217, (2016).
 - ¹³ Z. Yu and S. Fan, “Complete optical isolation created by indirect interband photonic transitions,” *Nature Photon.*, **3**, pp. 91-94, (2009).
 - ¹⁴ H. Lira, Z. Yu, S. Fan, and M. Lipson, “Electrically driven nonreciprocity induced by interband photonic transition on a silicon chip,” *Phys. Rev. Lett.*, **109**, 033901, (2012).
 - ¹⁵ S. Qin and Y. E. Wang, “Broadband parametric circulator with balanced monolithic integrated distributedly modulated capacitors (DMC),” in IEEE MTT-S Int. Microw. Symp. Dig., San Francisco, CA, USA, May 2016, pp. 1-3.
 - ¹⁶ D. L. Sounas, C. Caloz, and A. Alú, “Giant non-reciprocity at the subwavelength scale using angular momentum-biased metamaterials,” *Nat. Commun.*, **4**, p. 2407, (2013).
 - ¹⁷ N. A. Estep, D. L. Sounas, J. Soric, and A. Alú, “Magnetic-free non-reciprocity and isolation based on parametrically modulated coupled-resonator loops,” *Nature Phys.*, **10**, pp. 923-927, (2014).
 - ¹⁸ Y. Mazar, A. Alú, “One-Way Hyperbolic Metasurfaces Based on Synthetic Motion,” *arXiv:1902.02653* (2019)
 - ¹⁹ Y. Hadad, D. Sounas, and A. Alú, “Space-time gradient metasurfaces,” *Phys. Rev. B*, **92**, p. 100304(R), (2015).
 - ²⁰ Y. Hadad, J. C. Soric, and A. Alú, “Breaking temporal symmetries for emission and absorption,” *Proc. Natl. Acad. Sci.*, **10**, pp. 3471-3475, (2016).
 - ²¹ S. Taravati, N. Chamanara, and C. Caloz, “Nonreciprocal electromagnetic scattering from a periodically space-time modulated slab and application to a quasisonic isolator,” *Phys. Rev. B*, **96**, (16), (2017).
 - ²² S. Taravati and C. Caloz, “Mixer-Duplexer-Antenna Leaky-Wave System Based on Periodic Space-Time Modulation,” *IEEE Trans. Ant. Prop.*, **65**, (2), pp. 442-452, (2017).
 - ²³ H. Chalabi, Y. Radi, D. L. Sounas, and A. Alú, “Efficient anomalous reflection through near-field interactions in metasurfaces,” *Phys. Rev. B*, **96**, 075432, (2017).
 - ²⁴ Y. Radi, D. L. Sounas, A. Alu, “Metagratings: beyond the limits of graded metasurfaces for wave front control,” *Phys. Rev. Lett.*, **119**, (6), 067404, (2017).
 - ²⁵ A. Epstein, O. Rabinovich, “Unveiling the properties of metagratings via a detailed analytical model for synthesis and analysis,” *Phys. Rev. Appl.*, **8**, (5), 054037, (2017).
 - ²⁶ O. Rabinovich, A. Epstein, “Analytical Design of Printed-Circuit-Board (PCB) Metagratings for Perfect Anomalous Reflection,” *IEEE Trans. Antennas Propag.*, **66**, (8), pp. 4086-4095, (2018).
 - ²⁷ V. Popov, F. Boust, and S. N. Burokur, “Controlling Diffraction Patterns with Metagratings,” *Phys. Rev. Applied* **10**, 011002 (2018).
 - ²⁸ V. Popov, F. Boust, and S. N. Burokur, “Constructing the Near field and Far field with Reactive Metagratings: Study on the Degrees of Freedom,” *Phys. Rev. Applied* **11**, 024074 (2019).
 - ²⁹ V. Popov, F. Boust, S. N. Burokur, “Beamforming with metagratings at microwave frequencies: design procedure and experimental demonstration,” *arXiv:1904.13294* (2019).
 - ³⁰ A. Epstein, O. Rabinovich, “Perfect Anomalous Refraction with Metagratings,” *arXiv:1804.02362*, (2018).
 - ³¹ A. Diaz-Rubio, V. S. Asadchy, A. Elsakka, and S. A. Tretyakov, “From the generalized reflection law to the realization of perfect anomalous reflectors,” *Science Advances*, **3**, e1602714, (2017).
 - ³² S. Taravati, G. V. Eleftheriades, “Generalized Space-Time Periodic Diffraction Gratings: Theory and Applications,” *arXiv:1902.09885* (2019).
 - ³³ N. Yu, *et al.*, “Light propagation with phase discontinuities: Generalized laws of reflection and refraction,” *Science*, **334**, pp. 333-337, (2011).
 - ³⁴ F. Monticone, N. M. Estakhri, and A. Alú, “Full control of nanoscale optical transmission with a composite metascreen,” *Phys. Rev. Lett.*, **110**, 203903, (2013).
 - ³⁵ Y. Li, *et al.*, “Experimental realization of full control of reflected wave with subwavelength acoustic metasurfaces,” *Phys. Rev. Appl.*, **2**, 064002, (2014).
 - ³⁶ C. Pfeiffer and A. Grbic, “Millimeter-wave transmitarrays for wavefront and polarization control,” *IEEE Trans. Antennas Propag.*, **61**, pp. 4407-4417, (2013).
 - ³⁷ M. Selvanayagam and G. V. Eleftheriades, “Circuit modelling of Huygens surfaces,” *IEEE Antennas Wireless Propag. Lett.*, **12**, pp. 1642-1645, (2013).
 - ³⁸ M. Selvanayagam and G. V. Eleftheriades, “Discontinuous electromagnetic fields using orthogonal electric and magnetic currents for wavefront manipulation,” *Opt. Express*, **21**, pp. 14409-14429, (2013).
 - ³⁹ C. Pfeiffer and A. Grbic, “Metamaterial Huygens surfaces: tailoring wave fronts with reflectionless sheets,” *Phys. Rev. Lett.*, **110**, 197401, (2013).
 - ⁴⁰ D. Sevenpiper, J. Schaffner, R. Loo, G. Tangonan, S. Ontiveros, and R. Harold, “A tunable impedance surface performing as a reconfigurable beam steering reflector,” *IEEE Trans. Antennas Propag.*, **50**, pp. 384-390, (2002).
 - ⁴¹ E. Hasman, V. Kleoner, G. Biener, and A. Niv, “Polarization dependent focusing lens by use of quantized Pancharatnam Berry phase diffractive optics,” *App. Phys. Lett.*, **82**, p. 328, (2003).
 - ⁴² D. Lin, P. Fan, E. Hasman, and M. L. Brongersma, “Dielectric gradient metasurface optical elements,” *Science*, **345**, pp. 298-302, (2014).
 - ⁴³ J. P. S. Wong, M. Selvanayagam, and G. V. Eleftheriades, “Design of unit cells and demonstration of methods for synthesizing Huygens metasurfaces,” *Photonics and Nanos- tructures: Fundam. Appl.*, **12**, pp. 360-375, (2014).
 - ⁴⁴ M. Kim, A. M. H. Wong, and G. V. Eleftheriades, “Optical Huygens metasurfaces with independent control of the magnitude and phase of the local reflection coefficients,” *Phys. Rev. X*, **4**, 041042, (2014).
 - ⁴⁵ A. Epstein, G. V. Eleftheriades, “Huygens metasurfaces via the equivalence principle: design and applications,” *Journal of Opt. Soc. Am. B*, **33**, (2), pp. A31-A50, 2016.
 - ⁴⁶ A. Epstein, G. V. Eleftheriades, “Passive Lossless Huygens Metasurfaces for Conversion of Arbitrary Source Field to Directive Radiation,” *IEEE Trans. Antennas Propag.*, **62**, (11), pp. 5680-5695, (2014).
 - ⁴⁷ A. Epstein, J. P. S. Wong, G. V. Eleftheriades, “Cavity-excited Huygens metasurface antennas for near-unity aperture illumination efficiency from arbitrarily large apertures,” *Nature Commun.*, **7**, p. 10360, (2016).
 - ⁴⁸ A. H. Dorrah, M. Chen, G. V. Eleftheriades, “Bianisotropic Huygens Metasurface for Wideband Impedance Matching Between Two Dielectric Media,” *IEEE Trans. Antennas Propag.*, **66**, (9), pp. 4729-4742, (2018).
 - ⁴⁹ D. L. Sounas, N. M. Estakhri, and A. Alú, “Metasur-

- faces with engineered reflection and transmission: Optimal designs through coupled-mode analysis,” in 10th International Congress on Advanced Electromagnetic Materials in Microwaves and Optics - Metamaterials 2016, Crete, Greece, Sep. 2016.
- ⁵⁰ B. T. Draine and P. J. Flatau, “Discrete-dipole approximation for scattering calculations,” *J. Opt. Soc. Am. A* **11** (4) pp. 1491-1499 (1994)
 - ⁵¹ S. Tretyakov, *Analytical Modelling in Applied Electromagnetics*, Artech House, 2003.
 - ⁵² Y. Hadad, B. Z. Steinberg, “Quasistatic resonance of a chemical potential interruption in a graphene layer and its polarizability: The mixed-polarity semilocalized plasmon,” *Phys. Rev. B* **88** (7), 075439 (2013).
 - ⁵³ Y. Hadad, B. Z. Steinberg, “Magnetized spiral chains of plasmonic ellipsoids for one-way optical waveguides,” *Phys. Rev. Lett.* **105** (23), 233904 (2010).
 - ⁵⁴ Y. Mazar, B. Z. Steinberg, “Longitudinal chirality, enhanced nonreciprocity, and nanoscale planar one-way plasmonic guiding,” *Phys. Rev. B* **86** (4), 045120 (2012).
 - ⁵⁵ Y. Mazar, Y. Hadad, B. Z. Steinberg, “Planar one-way guiding in periodic particle arrays with asymmetric unit cell and general group-symmetry considerations,” *Phys. Rev. B* **92** (12), 125129 (2015).
 - ⁵⁶ In the following we apply the proposed approach on infinite wires excited by electromagnetic wave polarized along the wire axis. While the theory remains essentially the same, in this context a better term would be susceptibility rather than polarizability.
 - ⁵⁷ A. G. Hayrapetyanab, K. K. Grigoryanc, R. G. Petrosyanc, and S. Fritzschede, “Propagation of sound waves through a spatially homogeneous but smoothly time-dependent medium,” *Annals of Physics*, **333**, pp. 47-65 (2013).
 - ⁵⁸ A. G. Hayrapetyan, J. B. Gotte, K. K. Grigoryan, S. Fritzsche, and R. G. Petrosyan, “Electromagnetic wave propagation in spatially homogeneous yet smoothly time-varying dielectric media,” *Journal of Quantitative Spectroscopy and Radiative Transfer*, **178**, pp. 158-166 (2016).
 - ⁵⁹ A. G. Hayrapetyan, S. P. Klevansky, and J. B. Gotte, “Instantaneous modulations in time-varying complex optical potentials,” *New J. Phys.*, **19**, 105002 (2017).
 - ⁶⁰ A. Shlivinski and Y. Hadad, “Beyond the Bode-Fano Bound: Wideband Impedance Matching for Short Pulses Using Temporal Switching of Transmission-Line Parameters,” *Phys. Rev. Lett.* **121** (20), 204301 (2018).
 - ⁶¹ Y. Hadad, A. Shlivinski, “Soft Temporal Switching of TL Parameters: Wave-field, Energy Balance, Applications,” *arXiv:1905.02377* (2019).
 - ⁶² M. Liu, X. Yin, E. Ulin-Avila, B. Geng, T. Zentgraf, L. Ju, F. Wang, and X. Zhang, “A graphene-based broadband optical modulator,” *Nature*, **474**, pp. 64-67, (2011).
 - ⁶³ C. T. Phare, Y.-H. D. Lee, J. Cardenas, and M. Lipson, “Graphene electro-optic modulator with 30 GHz bandwidth,” *Nat. Photon.*, **9**, pp. 511-514, (2015).
 - ⁶⁴ M. A. Green, “Time-asymmetric photovoltaics,” *Nano Lett.*, **12**, pp. 5985-5988, (2012).
 - ⁶⁵ L. Zhu and S. Fan, “Near-complete violation of detailed balance in thermal radiation,” *Phys. Rev. B*, **90**, 220301, (2014).
 - ⁶⁶ Y. Hadad, B. Z. Steinberg, “Greens function theory for infinite and semi-infinite particle chains,” *Phys. Rev. B* **84** (12), 125402 (2011)
 - ⁶⁷ Y. Hadad, Y. Mazar, B. Z. Steinberg, “Green’s function theory for one-way particle chains,” *Phys. Rev. B* **87** (3), 035130 (2013).